JOURNAL OF MATERIALS SCIENCE 28 (1993) 6217–6221

Fracture toughness of discontinuously reinforced aluminium 6061 matrix composites

M. J. HADIANFARD, J. C. HEALY, YIU-WING. MAI
Centre for Advanced Materials Technology, Department of Mechanical and Mechatnonic Engineering, University of Sydney, New South Wales 2006, Australia

The fracture toughness of two aluminium 6061 matrix composites reinforced with 20 vol% discontinuous reinforcement has been determined over a range of heat treatments. The materials investigated were Comral-85, reinforced with 20 vol% alumina-based microspheres, and Duralcan reinforced with 20 vol% angular alumina particulates. These were produced in an identical manner. Although the fracture toughness of both materials was relatively insensitive to ageing time, the Duralcan composite was significantly tougher than Comral-85 for all heat treatments examined. The matrix composition of both alloys was determined and it was found that Comral-85 contained higher additions of silicon and iron, resulting in the formation of an increased density of secondary particles. This was found to be the primary cause of the difference in fracture toughness between these two materials.

1. Introduction

The addition of a discontinuous reinforcement phase to an aluminium matrix can significantly improve the strength and wear resistance when the properties are compared to those of the unreinforced alloy. The lower ductility, smaller tensile fracture strain and reduced fracture toughness [1–5] of metal matrix composites (MMCs) in comparison to their matrix alloys are major obstacles in the use of these materials in many applications. Whilst fracture toughness values for unreinforced aluminium alloys are in the range of 25–75 MPa $m^{1/2}$, MMCs have fracture toughness, K_{Ic}, values in the range 7–25 MPa $m^{1/2}$ [6]. In addition, many factors affect the fracture toughness of these materials resulting in a wide range of nominal K_Q values (which are not necessary valid K_{Ic} measurements). In discontinuously reinforced aluminium 6061-based composites, K_{Ic} values of between 7 and 29 MPa $m^{1/2}$ have been obtained [7, 8].

It is therefore important to understand the factors which govern the toughness of this class of composites. This study attempts to develop a clearer picture of the factors which influence the fracture toughness by investigating two materials of the same nominal matrix alloy, the same volume fraction of reinforcement and produced by the same route but with different toughness, and identifying the reasons for this difference.

2. Experimental procedure

2.1. Materials

Two materials were used in this study, Comral-85 and Duralcan 20 vol% Al_2O_3, Fig. 1a and b, respectively. They were supplied by Comalco Research Centre, Thomastown, Victoria, Australia, and produced by liquid metallurgy and extruded to 75 mm wide and 25 mm thick plates. Both materials had an aluminium 6061 matrix and 20 vol% alumina particulate reinforcement. The particulate morphology, determined from image analysis, is given in Table I. The reinforcement phases are very similar in size with the alumina in the Duralcan 20% being slightly larger and having a larger inter-particulate spacing. The main difference between these two phases is in the particulate shape, with spherical microspheres in the Comral-85 and angular alumina particles in the Duralcan 20%.

2.2. Heat treatment

Specimens were cut from the plates in the L–T orientation and subjected to the following heat treatments.

(a) Solution heat treated at 530 °C for 1.5 h.
(b) Cold-water quenched.
(c) Natural ageing for 24 h.
(d) Age hardening at 175 °C for time periods varying from 2–24 h.

The peak hardness (T6 condition) was achieved after 8 h at 175 °C [9].

2.3. Tensile tests

Tensile testing was performed using an 1195 Instron machine. A crosshead speed of 1 mm min^{-1} was used for all the tests and the load–elongation curves were recorded on an X–Y recorder. The Young's modulus, E, 0.2% offset yield, elongation to failure, ε_f, and ultimate tensile stress, UTS, were obtained in the T6 condition for both materials.

2.4. Fracture toughness tests, K_{Ic}

The fracture toughness tests were carried out on compact tension (CT) specimens with a width, W, of

0022–2461

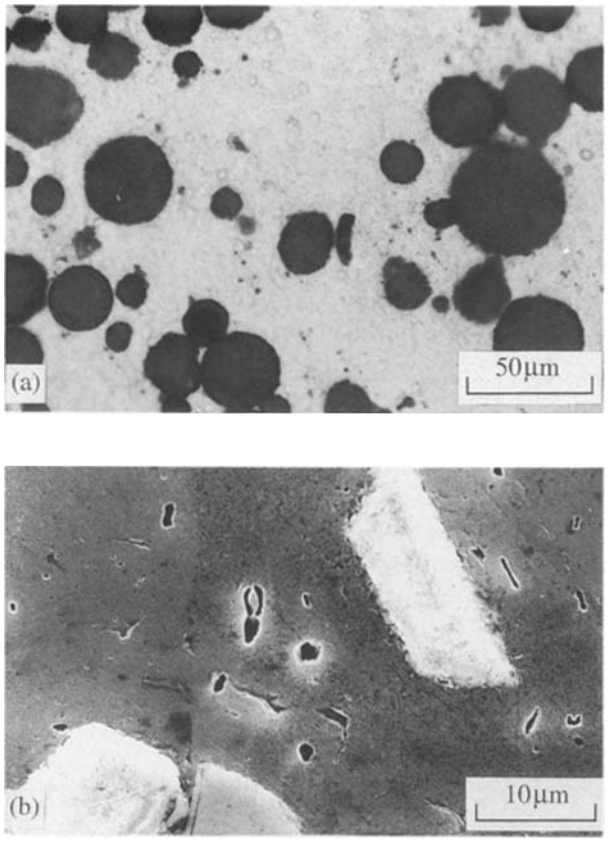

Figure 1 Polished and etched microstructures (1% hydrofluoric acid): (a) Comral-85; (b) Duralcan 20% alumina.

TABLE I Particulate morphology

Material (as-received and polished)	Average particle diameter (length) (μm)	Average interparticulate distance (μm)	Particle density (μm^{-1})
Comral-85	17.5	12.2	0.032
Duralcan 20%	18.7	14.6	0.025

50 mm in accordance with the ASTM Standard E399. Three tests were carried out on specimens in the under-aged (UA, 175 °C for 2 h), peak-aged (T6, 175 °C for 8 h) and over-aged (OA, 175 °C for 24 h) conditions. Precracking was performed using a 1603 Instron electro-magnetic resonator.

2.5. Chemical analysis

Matrix analysis was qualitatively determined using energy dispersive analysis of X-rays (EDAX) and quantitatively with the atomic absorption method by a Perkin–Elmer analyser with parts per million (p.p.m.) accuracy. The reinforcing and secondary particles present in both materials were also examined using EDAX analysis.

2.6. Fractography and image analysis

The fracture surfaces of peak-aged specimens were examined in the Phillips 505 and JSM Jeol scanning electron microscopes (SEM). The micrographs obtained were subjected to image analysis to quantify the fracture surface features and identify the fracture mechanisms.

3. Results

3.1. Tensile properties and fracture toughness

The room-temperature mechanical properties for the peak-aged condition are shown in Table II. These results indicate that Duralcan has both higher yield and tensile strengths than Comral-85. In addition the Young's modulus of Duralcan is 9% larger.

The fracture toughness values for the UA, T6 and OA heat treatments are given in Table III. The fracture toughness is seen to decrease slightly with increasing ageing time for both materials. However, it should be noted that this corresponds to a decrease of only 4% from UA to OA in Comral-85 and 9% in Duralcan. Thus the fracture toughness of both materials is relatively insensitive to ageing over the range 2–24 h at 175 °C.

Despite the same nominal aluminium matrix and volume fraction of reinforcement, the Duralcan material has a significantly higher fracture toughness in all heat treatments examined, 20% higher in the UA and T6 conditions, and 17% higher in the OA condition.

3.2. Chemical analysis

EDAX analysis of both matrices are presented in Fig. 2a and b. Although it is only a qualitative technique, it is clear that the Comral-85 matrix contains additions of scandium, titanium, chromium, iron and copper in quantities which are not present in the Duralcan matrix. Further EDAX analysis of the reinforcement phase shows that in Duralcan it contains pure alumina, whereas in Comral-85 the alumina microspheres contain additions of magnesium, silicon and iron. To quantify the differences in composition between the matrix of both materials, an atomic absorption technique was used, the results of which are presented in Table IV. Comral-85 has significantly higher additions of silicon, iron, chromium and titanium but a lower addition of magnesium. These

TABLE II Room-temperature mechanical properties, T6 condition

Material	Yield stress (MPa)	UTS (MPa)	E (GPa)	ε_f (%)
Comral-85	318 ± 4	346 ± 4.3	88.8 ± 2.3	3.66 ± 0.7
Duralcan 20%	335 ± 3.9	354 ± 2.3	97 ± 2.5	3.2 ± 0.4

TABLE III Fracture toughness of over-aged, peak-aged and under-aged composites

K_{Ic} (MPa $m^{1/2}$)		Condition	Heat treatment	
Comral-85	Duralcan 20%		(°C)	(h)
19.0 ± 0.5	23.6 ± 0.25	UA	175	2
18.5 ± 0.35	22.8 ± 0.2	T6	175	8
18.3 ± 0.51	21.7 ± 0.92	OA	175	24

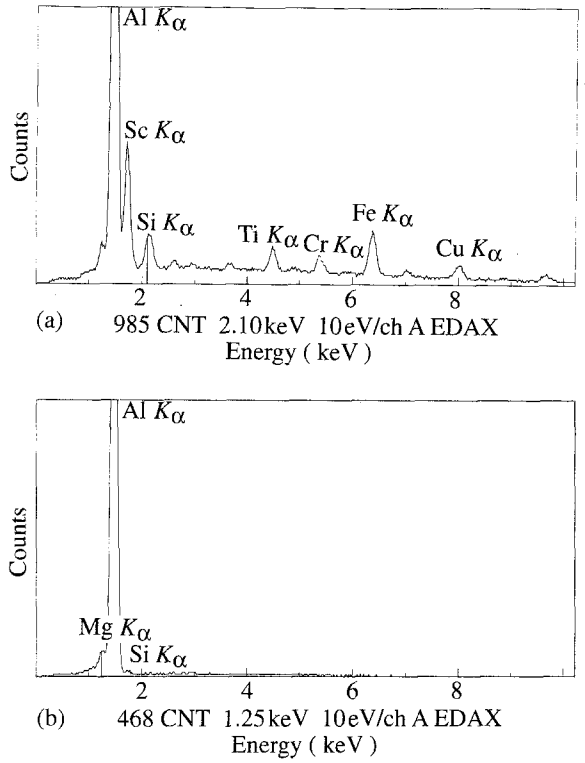

Figure 2 EDAX analysis of 6061 aluminium matrix: (a) Comral-85; (b) Duralcan 20%.

TABLE IV Matrix analysis obtained from atomic absorption

Material	Element (wt %)				
	Si	Fe	Mg	Cr	Ti
Comral-85	0.63	0.80	0.82	0.33	0.13
Duralcan 20%	0.41	0.36	1.12	0.15	0.08

differences have affected the amount and size of the secondary particles. In Comral-85 there was a large number of non-uniform secondary particles ranging in size from 8–15 μm. This is illustrated in the micrograph of the unreinforced matrix alloy used to manufacture Comral-85, Fig. 3. By comparison the Duralcan composite had a smaller amount of secondary particles with sizes between 5 and 10 μm. EDAX analysis of iron-rich particles shows that while they consist of aluminium and iron in Duralcan, those in Comral-85 consist of aluminium, silicon, iron and manganese.

3.3. Fractography and image analysis

The T6 fracture surfaces of both materials were subjected to detailed image analysis. Representative scanning electron micrographs of both materials are presented in Fig. 4a and b. The resulting analyses are presented in Tables V and VI. Cursory examination of Fig. 4a and b shows that although the fracture surfaces of both materials exhibit ductile fracture morphology consisting of void formation, growth and coalescence in the matrix phase, there are differences between the two fracture surfaces. The matrix of the Duralcan specimen shows extensive shear and is drawn out to

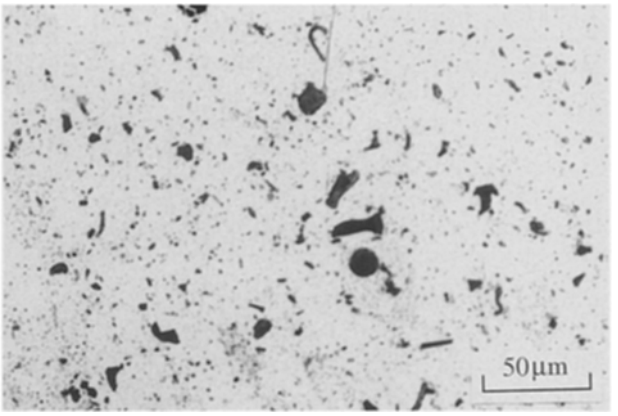

Figure 3 Polished and etched, microstructure of matrix alloy of Comral-85.

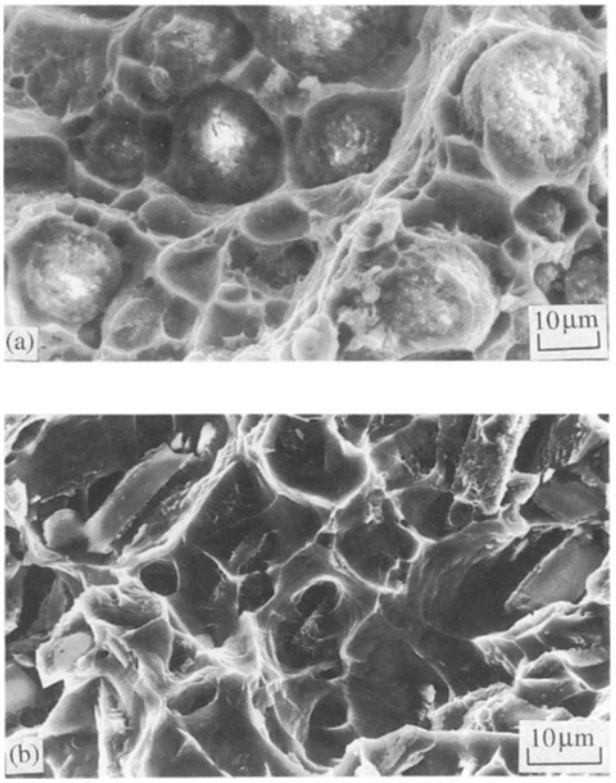

Figure 4 Fracture surface, T6 condition: (a) Comral-85; (b) Duralcan 20%.

TABLE V Fracture surface particulate morphology, T6 condition

Material fracture surface	Average fractured particles diameter (μm)	Area of fractured particles (%)	Inter-particulate spacing (μm)	% of fractured particles
Comral-85	19.8	7.5	9.2	40
Duralcan 20%	21.6	11.2	11.1	74

form a sharp shear lip between the alumina particles. The primary dimples around alumina particles are deep and a few small secondary dimples are visible. Although some separation of particles from the matrix was evident, most of particles were still firmly embedded in the matrix, Fig. 4b. In addition this material has

TABLE VI Fracture surface void characterization, T6 condition

Material	Type I voids Average diameter (μm)	Type II voids Average diameter (μm)	Type III voids Average diameter (μm)
Comral-85	16.9	6.7	1.5
Duralcan 20%	19.8	4.3	–

a higher percentage of fractured particles when compared to that of Comral-85 (74% compared to 40%). The fracture surface of Comral-85 is covered by a large number of shallow primary dimples and many small, shallow microvoids in the matrix, Fig. 4a, and there is significantly less visible drawing of the matrix. The fracture mechanism in Comral-85 is void coalescence, while in the Duralcan material there is less voiding but evidence of matrix shear failure is plentiful.

Three different populations of void sizes were observed on the fracture surface of Comral-85, Table VI, but only two were observed on the corresponding Duralcan fracture surface. The smallest population of voids, type III, with an average diameter of 1.5 μm was unique to Comral-85. It seems clear that these voids are due to the presence of a large number of secondary particles.

4. Discussion

Previous investigations of MMCs showed that factors such as the microstructure and deformation characteristics of the matrix, the morphology of the reinforcement and the properties of the matrix/particles (m/p) interface could affect significantly the fracture behaviour of these MMCs [3, 10, 11]. These same factors were also found to influence the fracture toughness behaviour of the materials studied in this work and they are discussed in turn below.

The fracture process occurs in distinct stages in each material. Firstly, large voids are nucleated by either the fracture of the large alumina particles or decohesion at the m/p interface resulting in type I voids (with diameter between 27 and 12 μm). The large number of fractured particles in the Duralcan composite compared to Comral-85 indicated that primary voids were nucleated around the fractured particles in Duralcan while they were initiated from the debonded m/p interface in Comral-85. Chemical analysis shows that the composition of the matrix, in addition to the reinforcement particles of these two materials, differs. It is not unreasonable, therefore, to assume that these differences can produce m/p interfaces with different strengths. The results of the image analyses indicate that the Comral-85 is more susceptible to fracture at the m/p interface than the Duralcan composite. Weak m/p interfacial bonding in Comral-85, produced by either different composition or secondary particles, causes damage to initiate at the interface in this material.

The voids initiated around particles are free to expand into the matrix by plastic deformation until they meet other voids. Further straining causes these microvoids to grow quickly. The small (between 2 and 10 μm) secondary particles between the large damaged alumina particles reduce the ductility of the Comral-85 matrix by producing types II (between 11 and 5 μm) and III voids (between 4 and 0.5 μm) and prevent further deformation. The comparatively pure matrix of Duralcan is free for further deformation resulting in deeper and larger dimples. The easy nucleation and propagation of microvoids near the iron-rich inclusions may be related to their weak strength. Low *et al.* [12] found one type of inclusion that mostly consisted of iron and silicon in an aluminium alloy. In ordinary tensile tests these particles began to fracture at 0.25% plastic strain. Metallographic studies of notched tensile bars revealed that the larger inclusions (0.1–10 μm iron-, silicon- and chromium-rich) began to crack shortly after the onset of plastic flow [10]. These constituent phases affect the failure mechanisms in the matrix ligament and contribute to the fracture toughness values observed for the composite.

The difference in particle morphology is another factor influencing the fracture mechanism. The angular reinforcement phase in Duralcan will have a higher stress concentration as compared to the spherical reinforcement in Comral-85. Thus there is an increased likelihood of particle fracture in Duralcan rather than separation from the interface and this partly explains why Comral-85 has more debonded particles.

Whilst the higher additions of iron, silicon and chromium in Comral-85 produce secondary particles which reduce the fracture toughness, the higher addition of magnesium in the Duralcan material makes it stronger and increases the yield strength. Because the amount of compound-forming elements (iron, silicon, chromium and titanium) is less in Duralcan, magnesium remains in the crystal structure of aluminium as a solute element and acts as a barrier for dislocation movement to increase the yield strength of this material. As the strength of the matrix increases, higher resistance in the matrix to plastic deformation occurs. This would increase the amount of energy required for void growth and is, therefore, another reason for the higher K_{Ic} obtained.

In summary the sequence of the fracture processes occurred as follows. Firstly, voids are nucleated by either cracking of the large alumina particles in Duralcan or decohesion at the m/p interface in Comral-85. Then, secondary voids are nucleated at iron-rich and medium-sized alumina particles in Comral-85. Finally, voids coalesce by either matrix deformation in Duralcan or tertiary voids that have nucleated at age-hardened precipitates in Comral-85 and eventual failure occurs. Thus an improvement in the ductility and K_{Ic} value of Comral-85 could be achieved by reducing void nucleation sites with removal of the secondary inclusions and by improving the m/p interfacial bond strength and/or toughness.

5. Conclusions

1. The fracture toughness of two aluminium 6061 matrix composites reinforced with 20 vol % discontin-

uous particulates was investigated. The fracture toughness of Duralcan 6061 with 20 vol % Al_2O_3 was found to be significantly higher than that of Comral-85, 6061 reinforced with 20 vol % alumina-based microspheres, for all heat treatments examined (i.e. under-aged, peak-aged and over-aged).

2. The fracture toughness of both materials was relatively insensitive to ageing at 175 °C, although the toughness decreased marginally with increasing ageing time.

3. The fracture mechanism in Comral-85 was found to be ductile failure based on dimple formation and microvoid coalescence; whereas the fracture mechanism in Duralcan 20% was a combination of matrix shear failure and void coalescence.

4. Although differences in particulate morphology may influence the fracture mechanisms, the primary reason for the higher fracture toughness values of Duralcan compared to Comral-85 are related to the significant differences in the composition of the matrix alloy. The Duralcan composite was found to have significantly less additions of iron and silicon which form secondary particles in Comral-85 providing preferential sites for void formation.

Acknowledgements

The supply of materials for testing from Comalco Research Centre is much appreciated. Financial support for this project was provided by the Australian Research Council Small Grants Scheme. M. Hadianfard also acknowledges the award of an ARC Junior Research Fellowship.

References

1. J. J. STEPHENS, J. P. LUCAS and F. M. HOSKING, *Scripta Metall.* **22** (1988) 1307.
2. W. G. LOGSDON and P. K. LIAW, *Eng. Fract. Mech.* **24** (1986) 737.
3. J. W. LEWANDOWSKI, C. LIU and W. H. HUNT, Jnr. in Proceedings of "Processing and Properties for Powder Metallurgy Composites", edited by P. Kumar, K. Vedula and A. Ritter (The Metals Society, Warrendale, PA, 1988) pp. 117–37.
4. Y. FLOM and R. J. ARSENAULT, *Acta. Metall.* **37** (1989) 2413.
5. M. MANOHARAN and J. J. LEWANDOWSKI, *ibid.* **38** (1190) 489.
6. R. D. GOOLSBY and L. K. AUSTIN, in "Proceedings of the International Congress on Fracture, 7", Vol. 4, edited by K. Salama, K. Ravi-Chandar, D. M. R. Taplin and P. Rama Rao (Pergamon Press, Oxford, 1989) pp. 2423–35.
7. C. M. FRIEND, *Mater. Sci. Technol.* **5** (1989) 1.
8. S. BANDYOPADHYAY, I. A. BURCH and R. MUSCAT, in "Proceedings of the Australian Fracture Group Symposium", Sydney, edited by Y. W. Mai (University of Sydney, Sydney, 1990) pp. 140–9.
9. M. J. HADIANFARD, Y. W. MAI and J. C. HEALY, *J. Mater. Sci.*, **28** (1993) 3665.
10. G. T. HAHN and R. ROSENFIELD, *Metall. Trans. A* **6** (1975) 653.
11. K. XIA and M. J. COPER, in "Proceedings of the Australian Fracture Group Symposium", Sydney, edited by Y. W. Mai (University of Sydney, Sydney, 1990) pp. 110–19.
12. J. R. LOW, R. H. VAN STON and R. H. MERCHANT, NASA TR NO2 NASA Grant 39-087-003 (1972).

Received 4 March
and accepted 27 April 1993